

# Conventional Radical and RAFT Alternating Copolymerizations of Hydroxyalkyl Vinyl Ethers and Dialkyl Maleates

Yan-Xin Zhang<sup>a</sup>, Dong Chen<sup>a</sup>, Gao-Fei Hu<sup>b</sup>, Yu-Hong Ma<sup>a\*</sup>, and Wan-Tai Yang<sup>a\*</sup><sup>a</sup> Beijing Engineering Research Center of Syntheses and Applications of Waterborne Polymers College of Materials Science and Engineering, Beijing University of Chemical Technology, Beijing 100029, China<sup>b</sup> Analytical and Testing Center, Beijing University of Chemical Technology, Beijing 100029, China Electronic Supplementary Information

**Abstract** The alternating copolymerization of hydroxyalkyl vinyl ethers and dialkyl maleates is investigated by conventional radical polymerization and reversible addition-fragmentation chain transfer polymerization (RAFT). The influence of comonomer structure, comonomer feeding ratios, and monomer concentrations on the copolymerization and the copolymer structure have been investigated systematically. With 2-hydroxyethyl vinyl ether (HEVE) and dimethyl maleates (DMM) as comonomers, a well-defined alternating copolymer is prepared with  $M_n=3400$  and  $M_w/M_n=1.93$  up to 71.6% monomer. The alternating sequential chain structure of the copolymers has been proved by both NMR and matrix-assisted laser desorption/ionization time-of-flight mass spectrometry (MALDI-TOF MS). The experimental reactivity ratios and theoretical calculated highest occupied molecular orbital and the lowest unoccupied molecular orbital of vinyl ethers and alkyl maleates support that these monomer pairs have tendency to form alternating copolymers. With 2-cyanopropan-2-yl *N*-methyl-*N*-(pyridin-4-yl)carbamodithioate as the RAFT agent, the molecular weight of HEVE and DMM copolymer increases with the monomer conversion, demonstrating a controlled radical polymerization feature with well-controlled molecular weight and relatively narrower molecular weight distribution. With alternating copolymer of HEVE and DMM as macro-CTA ( $M_n=5200$  and  $M_w/M_n=1.46$ ), both the chain extension with HEVE and DMM ( $M_n=10400$  and  $M_w/M_n=1.72$ ) and block copolymerization with vinyl acetate have been successfully achieved ( $M_n=8500$  and  $M_w/M_n=1.52$ ).

**Keywords** Radical polymerization; Vinyl ethers; Maleates; Alternating copolymer; RAFT polymerization

**Citation:** Zhang, Y. X.; Chen, D.; Hu, G. F.; Ma, Y. H.; Yang, W. T. Conventional radical and RAFT alternating copolymerizations of hydroxyalkyl vinyl ethers and dialkyl maleates. *Chinese J. Polym. Sci.* 2023, 41, 1856–1867.

## INTRODUCTION

The radical polymerization has been widely used in the mass production of industrial polymers due to its simple process and competitive cost. More than 50% of the annual output of the world synthetic plastics are produced by radical polymerization process, such as low-density polyethylene, poly(vinyl chloride), polystyrene, polyacrylates, and polyvinyl acetate. However, there are some vinyl derivatives, such as vinyl ethers and higher  $\alpha$ -olefins, are hardly undergo radical homopolymerization due to the steric or electron effects.<sup>[1]</sup> For example, the addition products of the radicals with vinyl ethers ( $\sigma$ -radicals) are highly reactive and unstable due to the adjacent alkoxy group (electron donor) lack of resonance stability.<sup>[2,3]</sup> Thus, the vinyl ether radical readily takes place unfavorable side reactions, such as  $\beta$ -scission and frequent hydrogen abstraction.<sup>[4,5]</sup> As a result, vinyl ethers are hardly proceeded *via* radical

homopolymerization to produce high molecular weight polymers.<sup>[2,4,6]</sup>

Considering their electron-rich nature,<sup>[5,7]</sup> poly(vinyl ether)s of high molecular weights are mainly prepared by cationic polymerization. The living cationic polymerization of alkyl vinyl ethers, first reported by Higashimura *et al.*<sup>[8]</sup> in 1984, have been successfully applied in synthesis of poly(vinyl ether)s with well-defined architectures.<sup>[9]</sup> Recently, the stereoregular polymerization, a true breakthrough, of cationic polymerization of vinyl ethers was reported by Leibfath *et al.*<sup>[10,11]</sup> Nevertheless, cationic polymerization is intolerable to the polar groups, such as hydroxyl and carboxyl groups. In addition, cationic polymerization always requires harsh reaction conditions, for instance, high purity of reactants and inert environment, which limit its industrial development.

In terms of mechanism, as long as the electron density of the  $-C=C-$  of vinyl ether can be adjusted, it is possible to realize the radical homopolymerization of vinyl ether. After continuous efforts, some achievements have been made on the radical homopolymerization of vinyl ethers in recent. For example, at pH=10.02, the radical homopolymerization of poly(oligoethylene glycol methyl vinyl ether) was demon-

\* Corresponding authors, E-mail: [mayh@mail.buct.edu.cn](mailto:mayh@mail.buct.edu.cn) (Y.H.M.)

E-mail: [yangwt@mail.buct.edu.cn](mailto:yangwt@mail.buct.edu.cn) (W.T.Y.)

Received February 14, 2023; Accepted April 7, 2023; Published online May 18, 2023

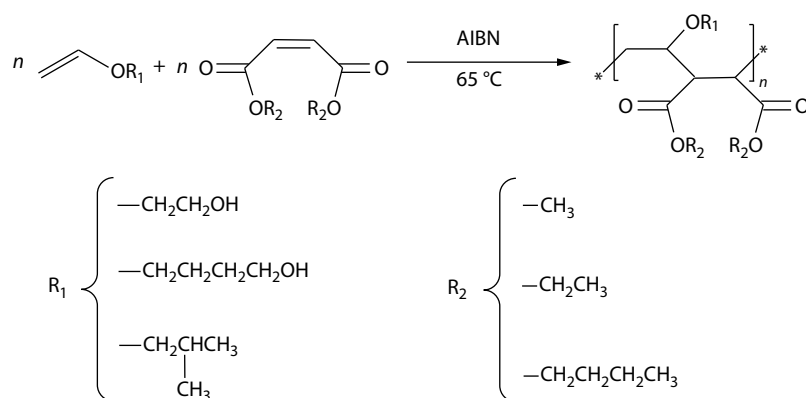
strated a highest  $M_n$  ever of 6600 and 7% conversion.<sup>[4]</sup> In 2016, Sugihara *et al.*<sup>[5]</sup> synthesized poly(hydroxyvinyl ether)s using dimethyl 2,2'-azobis(isobutyrate) as an initiator *via* bulk polymerization. Among them, poly(2-hydroxyethyl vinyl ether) was produced with  $M_n=26400$  ( $M_w/M_n=2.23$ ) and in high yield ( $\geq 75\%$ ). In 2019, a radical homopolymerization realized by complexation with LiOH in aqueous solution or hydrogen bonding in bulk polymerization has been introduced.<sup>[12]</sup> The  $\pi$  complexation of  $-C=C-$  with proper hydrogen bond and  $Li^+$  is the key to the free radical polymerization of vinyl ethers. In our recently work, we prepared a surface-grafted brush layer of poly(vinyl ether)s directly by UV-assisted radical grafting polymerization with  $CH_3OLi$  as a mediator.<sup>[13]</sup> Moreover, we also realized a direct, thermally initiated radical homopolymerization of vinyl ethers mediated by lithium salts  $CH_3OLi$  and  $LiI$ .<sup>[14]</sup> Although it has been proved that vinyl ethers are capable of free radical homopolymerization through the mediation of lithium salt or hydrogen bond, molecular weight and conversion of homopolymerization of vinyl ethers are still to be improved.

As a typical electron donor, vinyl ethers are easily to form charge-transfer complex (CTC) with electron acceptors to produce alternating copolymers. Hao *et al.*<sup>[15]</sup> reported that the copolymers of isobutyl vinyl ether (IBVE) and maleic anhydride (MA) were completely alternating and the proportion of the *cis* linkage configuration at the cyclic MA unit was  $48\pm 4\%$  in all copolymers regardless of the polymerization condition. Ha *et al.*<sup>[16]</sup> found that both copolymers were made of completely alternating monomer unit sequences and that the proportion of *cis* linkage configuration at the cyclic MA units was 45% and 47% in the copolymers of 2-chloroethyl vinyl ether-maleic anhydride and *n*-butyl vinyl ether-MA respectively. Maleates, 1,2-disubstituted ethylene derivatives with electron-withdrawing groups, are typical electron acceptors and non-radical homopolymerizable monomers.<sup>[17–19]</sup> It makes them have potential to substitute maleic anhydride which copolymerizes with electron-rich monomers such as styrene, vinyl ethers, furan and 2-methylfuran to prepare alternating copolymers by radical copolymerization.<sup>[20–22]</sup>

Considering the poor control of polymerization degree and molecular weight distribution of polymers by conventional radical polymerization, reversible deactivation radical polymerization (RDRP) has become a robust tool in macromolecular architecture design. Nowadays, the widely applied RDRPs

mainly include nitroxide-mediated polymerization (NMP),<sup>[23]</sup> atom transfer radical polymerization (ATRP),<sup>[24–26]</sup> reversible addition-fragmentation chain transfer (RAFT).<sup>[27–29]</sup> Among them, RAFT is applicable to broad monomers and tolerant to functional groups. Zhang *et al.*<sup>[30]</sup> synthesized poly(styrene-*alt*-maleimide isobutyl POSS) copolymer by RAFT polymerization. Alternating RAFT copolymerization of styrene and maleic anhydride with molecular weight distribution ( $M_w/M_n$ ) as low as 1.19 has also been studied for a long time.<sup>[31]</sup> Lee *et al.*<sup>[32]</sup> synthesized poly(vinyl acetate-*alt*-dibutyl maleate) (PVAc-*alt*-PDBM) copolymer by RAFT polymerization using xanthate as mediator. In 2017, Sugihara *et al.*<sup>[33]</sup> prepared poly(HEVE-*co*-VAc) and alkali-hydrolyzed poly(HEVE-*co*-VA) by RAFT radical copolymerization. Puts *et al.*<sup>[34]</sup> realized radical copolymerization of tetrafluoroethylene and IBVE in dimethyl carbonate, with *O*-ethyl-*S*-(1-methyloxycarbonyl)ethyl xanthate as RAFT agent.

In this contribution, we studied the radical copolymerization of vinyl ethers and dialkyl maleates by both conventional radical and RAFT polymerizations. The formation of hydrogen bonding among hydroxyalkyl vinyl ethers can significantly improve the homopolymerization reactivity and the hydroxyl groups in the copolymer chains offer post-polymerization reactivity. The polymerization experiments were carried out with different vinyl ether monomers, including 2-hydroxyethyl vinyl ether (HEVE), 4-hydroxybutyl vinyl ether (HBVE) and IBVE, and maleates such as dimethyl maleate (DMM), diethyl maleate (DEM) and dibutyl maleate (DBM) (Scheme 1). All the copolymers of hydroxyalkyl vinyl ethers and maleates have alternating sequential structures. The impacts of the monomer feed ratio, solvents, monomer concentration and other factors on the copolymerization of vinyl ethers and maleates were systematically investigated. With the successful synthesis of alternating copolymers by conventional radical polymerization, the RAFT copolymerization of vinyl ethers and maleates was also exploited with 2-cyanopropan-2-yl *N*-methyl-*N*-(pyridin-4-yl)carbamidithioate as a mediator. The results demonstrated that the molecular weights of copolymers increased linearly with the monomer conversion and remained relatively narrow molecular weight distribution. In addition, we demonstrated block copolymerization with vinyl acetate (VAc) using poly(HEVE-*alt*-DMM) macromolecular chain transfer agent (macro-CTA). A novel alternating copolymer of vinyl ethers and dialkyl maleates with facile



**Scheme 1** Monomers of vinyl ethers and maleates used in the study.

method and tailoring structure reported in this contribution offers an option how to use the 1,2-disubstituted ethylene to prepare high value functional/reactive polymers. And these copolymers are expected to find applications in polyurethanes, adhesive and low VOC coating formulations.

## EXPERIMENTAL

### Materials

2-Hydroxyethyl vinyl ether (HEVE,  $\geq 98.0\%$ , Macklin), 4-hydroxybutyl vinyl ether (HBVE,  $\geq 98.0\%$ , Macklin), isobutyl vinyl ether (IBVE, stabilized with KOH,  $> 99.0\%$ , TCI), dimethyl maleate (DMM,  $\geq 98.0\%$ , Macklin), diethyl maleate (DEM,  $\geq 96.0\%$ , Aladdin) and dibutyl maleate (DBM,  $\geq 97.0\%$ , Aladdin), 2,2'-azobisisobutyronitrile (AIBN,  $\geq 99.0\%$ , Macklin), benzoyl peroxide (BPO,  $\geq 97.0\%$ , Alfa Aesar, recrystallization), dimethyl carbonate (DMC,  $\geq 99.0\%$ , Macklin), ethanol ( $\geq 99.7\%$ , Fuyu Fine Chemical), methanol ( $\geq 99.7\%$ , Fuyu Fine Chemical), isopropanol (IPA,  $\geq 99.7\%$ , Damao Chemical Reagent), methyl *tert*-butyl ether (MTBE,  $\geq 99.0\%$ , Fuchen Chemical), 2-mercaptoethanol (BME,  $\geq 99.0\%$ , J&K Chemicals), thioglycolic acid (TGA,  $99.0\%$ , J&K Chemical), isoamyl acetate ( $99.0\%$ , Fuchen Chemical), tetrahydrofuran (THF, HPLC grade, MREDA), chloroform- $d_3$  ( $CDCl_3$ ,  $99.8\%$  D, Macklin, with  $0.1\%$  TMS), acetone- $d_6$  ( $C_3D_6O$ ,  $99.8\%$  D, Macklin, with  $0.1\%$  TMS), (methyl sulfoxide)- $d_6$  ( $DMSO-d_6$ ,  $99.8\%$  D, Macklin, with  $0.1\%$  TMS), 2-cyanopropan-2-yl *N*-methyl-*N*-(pyridin-4-yl)carbamodithioate ( $97\%$ , HPLC grade, Sigma-Aldrich), vinyl acetate (VAc,  $98\%$ , Macklin) were used as received.

### Conventional Radical Copolymerization

The conventional radical copolymerization of vinyl ethers and maleates was carried out at  $65\text{ }^\circ\text{C}$  with equal molar ratio and 30 wt% total monomer concentration, 1.0 wt% AIBN (on total monomers) as initiator and DMC as solvent. All reagents were added to a single-neck round-bottom flask and immersed in a preheated oil bath. For example, the reactant was conducted under stirring for 12 h to obtain the sample. After polymerization, the copolymers were precipitated with MTBE. The as-prepared copolymer was dried in a vacuum oven for subsequent characterization.

### RAFT Polymerization

For comparison, the types and concentrations of monomers, initiator and solvent are consistent with those of conventional radical polymerization. Furthermore, all the reactants, for example, 1.16 g of HEVE (13.22 mmol), 1.90 g of DMM (13.22 mmol), 99.7 mg of RAFT agent (0.39 mmol), 21.7 mg of AIBN (0.13 mmol), 7.2 g of DMC (70 wt%), and 3.1 g of isoamyl acetate,  $[HEVE]_0/[DMM]_0/[RAFT\ agent]_0/[AIBN]_0=100/100/3/1$ , were introduced into a flask. Then, oxygen was removed by three freeze-pump-thaw cycles, and finally the flask was filled with argon and immersed in a preheated oil bath. The reaction was conducted with stirring at  $65\text{ }^\circ\text{C}$ . The polymerization was quenched *via* rapid cooling in an ice-bath and exposure to air after the desired reaction time. After polymerization, washed with MTBE, ethanol and methanol for several times, then copolymer product was separated from the solution. The as-prepared copolymer was dried in a vacuum oven for subsequent characterization.

### Synthesis of Block Copolymers Using Macromolecular RAFT Agent (Macro-CTA)

Macro-CTA obtained by RAFT radical copolymerization was mixed with AIBN and VAc in a flask. The typical contents for poly(HEVE-*alt*-DMM)-*b*-poly(VAc) are as follows. VAc (0.33 g, 3.85 mmol), poly(HEVE-*alt*-DMM) macro-CTA ( $M_n=5200$ , 0.2 g, 38.46  $\mu\text{mol}$ ), AIBN (2.53 mg, 15.38  $\mu\text{mol}$ ), 0.77 g of DMC (70 wt%), and 0.31 g of isoamyl acetate,  $[VAc]_0/[poly(HEVE-*alt*-DMM)\ macro-CTA]_0/[AIBN]_0=100/1/0.4$ , were introduced into a flask. Then, oxygen was removed by three freeze-pump-thaw cycles, and finally the flask was filled with argon and immersed in a preheated oil bath. The reaction was conducted with stirring at  $65\text{ }^\circ\text{C}$ . The polymerization was quenched *via* rapid cooling in an ice-bath and exposure to air after the desired reaction time. After polymerization, washed with MTBE, ethanol and methanol for several times, then copolymer product was separated from the solution. The as-prepared copolymer was dried in a vacuum oven for subsequent characterization.

### Copolymer Characterizations

The number-average molecular weight ( $M_n$ ) and molecular weight distribution ( $M_w/M_n$ ) were assessed by a PL-GPC50 instrument (GPC) equipped with two polystyrene gel columns PLgel 5  $\mu\text{m}$  MIXED-C columns in series and a PL refractive-index detector using tetrahydrofuran as eluent. The  $^1\text{H-NMR}$  and  $^{13}\text{C-NMR}$  spectra were performed with a Bruker Avance III NMR spectrometer operating at 600.13 MHz ( $^1\text{H}$  frequency) in  $CDCl_3$ ,  $C_3D_6O$  and  $DMSO-d_6$  at  $25\text{ }^\circ\text{C}$ . The  $^1\text{H-NMR}$  (600.13 MHz,  $C_3D_6O$ , ppm) of the copolymers with initial feed ratio of HEVE/DEM=1/1 and HEVE/DBM=1/1 is reported in Fig. S5 (in the electronic supplementary information, ESI): (a) 4.02 ( $-\text{OCH}_2\text{CH}_3$ ); 3.44 ( $-\text{CH}_2\text{CH}-\text{OCH}_2\text{CH}_2\text{OH}$ ); 2.30–3.14 ( $-\text{CH}-\text{CH}-$ ); 1.46–2.20 ( $-\text{CH}_2\text{CH}-$ ); 1.16 ( $-\text{OCH}_2\text{CH}_3$ ); (b) 3.97 ( $-\text{OCH}_2\text{CH}_2\text{CH}_2\text{CH}_3$ ); 3.44 ( $-\text{CH}_2\text{CH}-\text{OCH}_2\text{CH}_2\text{OH}$ ); 2.31–3.18 ( $-\text{CH}-\text{CH}-$ ); 1.75 ( $-\text{CH}_2\text{CH}-$ ); 1.54 ( $-\text{OCH}_2\text{CH}_2\text{CH}_2\text{CH}_3$ ); 1.31 ( $-\text{OCH}_2\text{CH}_2\text{CH}_2\text{CH}_3$ ); 0.85 ( $-\text{OCH}_2\text{CH}_2\text{CH}_2\text{CH}_3$ ). To determine the monomer conversion of conventional copolymerization by gas chromatography (GC),<sup>[35]</sup> isoamyl acetate used as the internal standard should also be added. GC analysis was carried out on a GC-2014 (Shimadzu) gas chromatograph equipped with an RTX-1 capillary column (30 m  $\times$  0.25 mm  $\times$  0.25  $\mu\text{m}$ ) and a hydrogen flame ionization detector (FID), using nitrogen as carrier gas. Figs. S1 and S2 (in ESI) are the calibration curves of monomers (the peak area ratio of each monomer to isoamyl acetate in GC chromatograms). Matrix-assisted laser desorption/ionization time-of-flight mass spectrometry (MALDI-TOF MS) was acquired with an AB Sciex 5800 mass spectrometer with a nitrogen laser ( $\lambda=337\text{ nm}$ ) operated in the positive linear mode. Dissolved about 2 mg of the copolymer in 1 mL of THF and put it into a vial. The solution for MALDI-TOF MS analysis was obtained by mixing 2,5-dihydroxybenzoic acid matrix (10 mg/mL), and copolymer solution in a 1/1 (V/V). Then, 1  $\mu\text{L}$  of the mixture was analysed on MALDI-TOF MS in the positive-ion mode.

## RESULTS AND DISCUSSION

### Alternating Radical Copolymerization of Vinyl Ethers and Maleates

In order to understand the copolymerization of HEVE and DMM,

a series of reactions with different initial monomer feed ratios,  $[\text{HEVE}]_0/[\text{DMM}]_0=0.8/1, 1/1, 1.2/1$  (W/W), were carried out with 1.0 wt% AIBN, 70 wt% DMC as solvent, at 65 °C for 12 h. Fig. 1(a) presents the overall monomer conversions versus polymerization time. The kinetic curves of the copolymerization of HEVE and DMM demonstrate a typical radical polymerization. The monomer conversions increase sharply at the early stage (time less than 6 h) and then showed a levelling-off (from 6 h to 12 h). The highest overall monomer conversion was achieved at the equal monomer molar ratio. Electron donor/acceptor monomer pairs are easier to form CTCs when the feeding ratio is 1/1. The initial monomer feeding ratios also have some influences on the molecular weight of copolymers (Fig. 1b). With the increasing HEVE/DMM initial feeding ratio, the molecular weight of copolymers also increases. When the fraction of electron-donating monomers in the reactants increases, the interaction between electron donors and electron acceptors strengthens, which enhances the electron-accepting capability of DMM and thus improves the alternating copolymerization reactivity of HEVE and DMM. As a result, the molecular weight of the copolymer increases.

The copolymers were characterized by NMR and MALDI-TOF MS to further verify whether they are alternating copolymers. Fig. 2(a) shows  $^1\text{H-NMR}$  spectrum of the copolymer of HEVE and DMM with initial monomer feed ratio of 1/1. The broad peak at 3.22–4.21 ppm (1, 2, 3, 6 and 8) is ascribed to the  $-\text{OCH}_3$  of DMM,  $-\text{CH}-$ ,  $-\text{CH}_2\text{O}-$  and  $-\text{CHO}-$  of HEVE unit, respectively. The composition of the copolymer could be calculated by the area ratio of  $-\text{CH}-$  of DMM (5 and 7) and the  $-\text{CH}_2-$  (4) of HEVE in the backbone. The ratio is 1.04/1, very close to the theoretical 1/1 of alternating copolymer. The  $^{13}\text{C-NMR}$  spectrum of copolymer with 1/1 initial feed ratio is shown in Fig. 2(b). The signal around 74.38–80.24 ppm (1) is attributed to the  $-\text{CH}-$  of HEVE backbone, and the region of 70.44–73.71 ppm (2 and 3) belongs to the  $-\text{CH}_2-$  which is on the side groups of HEVE unit. Besides, the carbon peaks of  $-\text{CH}_2-$  and two  $-\text{CH}-$  on the main chain correspond to 32.24 ppm (4), 38.53–45.24 ppm (5), 50.41 ppm (8) in Fig. 2(b), respectively. The peaks at 170.08–175.22 ppm correspond to 6 and 9, while 7 and 10

peaks at about 51.58 and 60.99 ppm, respectively. This is mainly because the two pendants of DMM which are affected by the ether bond of HEVE. The heteronuclear single quantum coherence (HSQC) spectrum of the copolymers with initial feed ratio of HEVE/DMM=1/1 and  $^1\text{H-NMR}$  spectra of copolymers with different initial monomer feed ratios are shown in Figs. S3 and S4 (in ESI). There is no observable difference of the related chemical shifts, it can be inferred that difference of monomer ratio has no effect on the composition and sequential structure of the copolymer. It further supports that the copolymers of vinyl ethers and maleates are alternating.

The MALDI-TOF MS spectrum of the copolymer (HEVE/DMM=1/1) is represented in Fig. 3(a). A series of products with the molecular weight difference of 232.21 Da which is very close to the HEVE and DMM (232.24 Da) can be observed. For example, when the degree of polymerization of the copolymer is 10 ( $n=10$ ), the theoretical molecular weight of the oligomer (with alternating composition) should be 2322.4 Da ( $n=10$ ). The experimental value is 2428.65 Da, which is 106.25 Da more than the theoretical value. This 106.25 Da difference is the sum of the  $-(\text{CH}_3)_2\text{C}(\text{CN})-$  of the fragment of initiator AIBN and the polymer attached a  $\text{K}^+$  cation.<sup>[36]</sup> The error between the measured molecular weight and theoretical molecular weight of polymer fragments at different polymerization degrees is  $\pm 0.08$  Da, indicating that the measured results are considerably accurate. Simultaneously, the interval between adjacent fragments is near 88 and 144, respectively, which is just close to the theoretical molecular weight of HEVE and DMM monomer units. Fig. 3(b) displays the results of copolymers prepared with HEVE and DMM feed ratios of 0.8/1 and 1.2/1. A similar result could be observed. This indicates that the variation in the initial feed ratio does not change the alternating structure of the produced copolymers. In case of the same polymerization mechanism, copolymers of different maleates (DEM and DBM) and vinyl ethers (HEVE and HBVE) also have alternating structure (please refer to Figs. S5 and S6 in ESI).

The composition of the copolymer is largely determined by the monomer reactivity ratio and the reaction

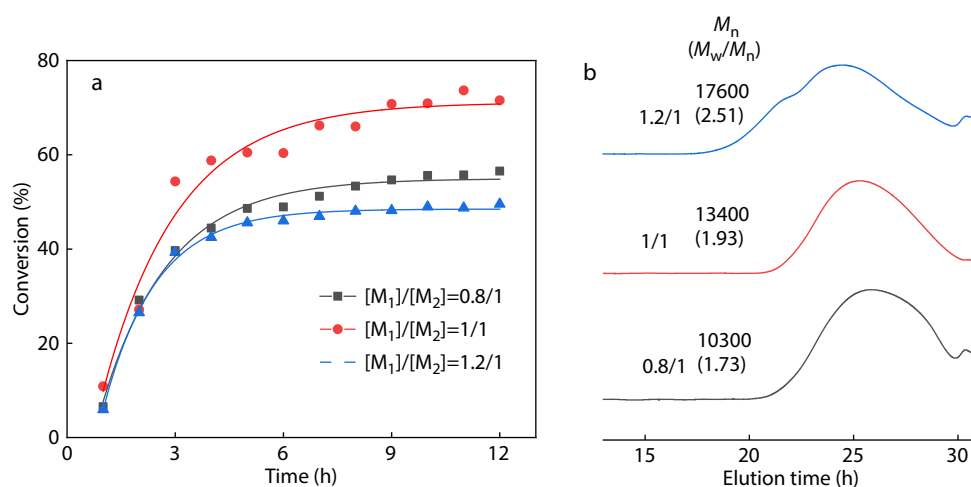


**Fig. 1** (a) Curves of overall monomer conversions versus polymerization time at different feed ratios ( $[\text{M}_1]/[\text{M}_2]=\text{HEVE}/\text{DMM}$ ); (b) GPC traces of copolymers with different initial monomer ratios.

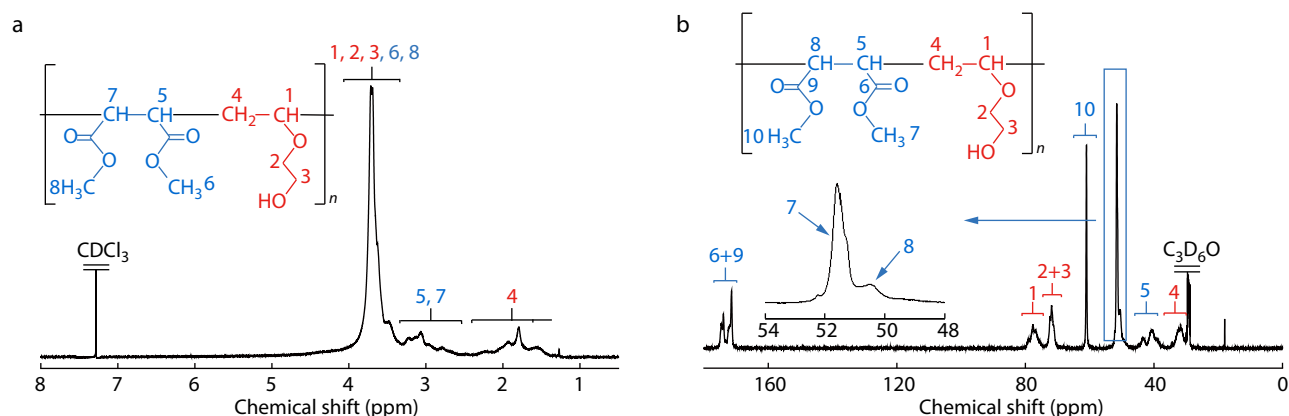


**Fig. 2** (a) <sup>1</sup>H-NMR and (b) <sup>13</sup>C-NMR spectra of the copolymer with initial feed ratio of HEVE/DMM=1/1 (molar ratio).

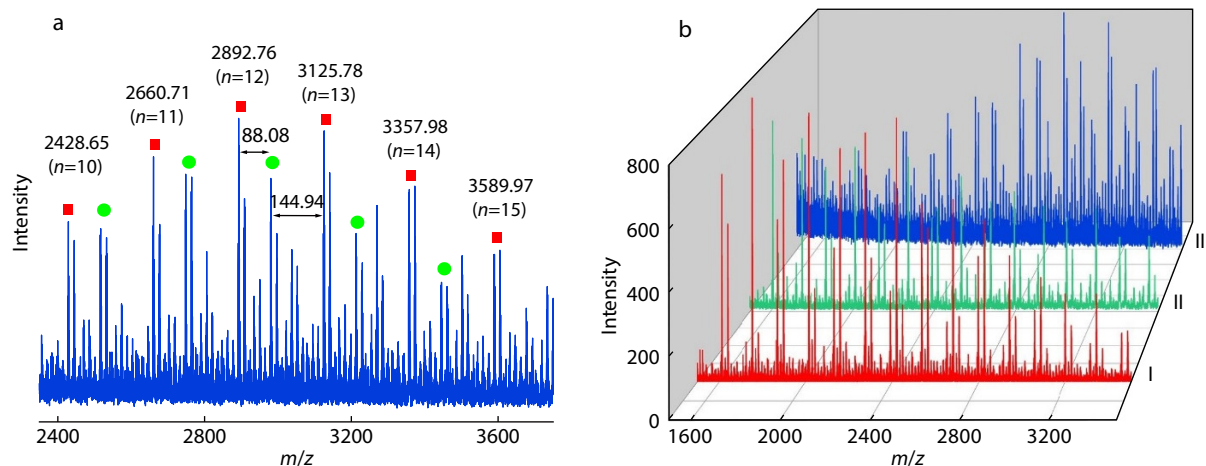


**Fig. 3** (a) MALDI-TOF MS spectrum of copolymer with initial monomer feed ratio of HEVE/DMM=1/1 (molar ratio); (b) MALDI-TOF MS spectra of copolymers with different initial monomer feed ratios: (I) HEVE/DMM=0.8/1; (II) HEVE/DMM=1.2/1; and (III) HEVE/DMM=1/1.

temperature.<sup>[37]</sup> The relative reactivity is the ratio of the self-growth rate constant to the cross-rate constant of the comonomer. Although the instantaneous composition of the copolymer cannot be determined directly, the composition of the copolymer at a low monomer conversion could be approximately taken as the instantaneous composition of the copolymer. By changing the monomer feed ratio, the composition of residual monomers in the solution at low conversion is determined by gas chromatography. The copolymer composition could be calculated with the monomer concentrations. Then the relative reactivity can be calculated by Fineman-Ross empirical method (Eqs. S1–S4 in ESI).<sup>[38]</sup>

Fig. S7 (in ESI) shows the results of relative reactivity. After fitting the experimental data, it was calculated that  $r_1(\text{HEVE}) = 0.11 \pm 0.07$ ,  $r_2(\text{DMM}) = 0.24 \pm 0.10$ , and the product of  $r_1 \times r_2 = 0.026$  is close to 0. When the product of  $r_1$  and  $r_2$  equals 0, the polymerization tends to alternating copolymerization.<sup>[39]</sup> The  $r_1$  and  $r_2$  also support that HEVE and DMM is an alternating copolymerization.

Copolymers with alternating structure (-DADADA-) can usually be obtained by binary molecules mixed stacking of CTC composed of  $\pi$ -electron donor (D) and  $\pi$ -acceptor (A).<sup>[40]</sup> To elucidate the copolymerization mechanism whether HEVE

and DMM can form a hybrid molecular complex between donor and acceptor (D-A complex) with partial CTC character,<sup>[41–44]</sup> the molecular geometries and electronic density distributions are simulated using density functional theory (DFT) at the B3LYP/6-31G (d) level using Gaussian 09 software package in Fig. 4. The highest occupied molecular orbital (HOMO) as an electron donor represents the ability to donate an electron and the lowest unoccupied molecular orbital (LUMO) acts as an electron acceptor which accepts an electron.<sup>[45]</sup> The HOMO and LUMO energy levels of HEVE are  $-5.88$  and  $1.14$  eV, respectively, which indicates that HEVE is an excellent electron donor. Meanwhile, the gap between the HOMO and LUMO of HEVE monomer is large, which also means it has high chemical stability, and difficult to homopolymerize.<sup>[46–49]</sup> Similarly, DMM is also an appropriate electron acceptor which is difficult to homopolymerize too. According to the frontier molecular orbital theory proposed by Fukui,<sup>[46]</sup> the electrons flow from the HOMO of molecules A<sub>1</sub> and A<sub>2</sub> to each other's unoccupied LUMO, causing the formation and fracture of chemical bonds. Only when the energy of HOMO of molecule A<sub>1</sub> (or A<sub>2</sub>) is close to that of LUMO of molecule A<sub>2</sub> (or A<sub>1</sub>), the electron flow is easy to occur when chemical reaction takes place. While for HEVE and DMM, the

electron flow direction is illustrated in Fig. 4. When two monomers are calculated in the same plane, it can be observed that the charge density is mainly accumulated on the electron donor in the HOMO(B) and on the electron acceptor in the LUMO(B). HOMO(B) and LUMO(B) are reduced by the influence of another molecule respectively, which indicates that the ability to donate electron or accept electron is enhanced.

The molecular electrostatic potential surface (MEPS) indicates the charge transfer effect of molecules and the electrophilic and the nucleophilic sites in the molecules where chemical reactions take place.<sup>[45,48]</sup> Fig. 5 shows the 3D MEPS of the monomers, calculated by the DFT method (B3LYP) and basis set (6-31G, d) for geometry optimization. The MEPS contour plots were extracted from the total self-consistent field density. The color schematic for the MEP surface (a) is as follows: blue for electron-rich (negative charge), red for electron-deficient (positive charge), and green for neutral (zero potential). For easy distinction, the color schematic for the MEP surface (b) is the opposite. In Fig. 5(a), the negative charge region attributed from the —OH group of the donor. From MEPS of DMM, in Fig. 5(b), the positive charge is mainly

concentrated at —C=C— and —CH<sub>3</sub> groups. These results also support the stronger electron donor ability of hydroxy vinyl ethers than alkyl vinyl ethers.<sup>[50]</sup> It further demonstrates the alternating structure of poly(HEVE-*alt*-DMM).

### Effects of Reaction Parameters on the Copolymerization of Vinyl Ethers and Maleates

#### Effect on monomer conversions

Copolymerization of vinyl ethers and maleates at different reaction conditions is presented in Fig. 6 and Table S1 (in ESI). Fig. 6(a) plots the relationship between reaction conversions and initiator concentrations. Except at 0.5 wt% AIBN (on total monomers), the monomer conversions increase monotonously with the evolution of the polymerization and tend to levelling-off at long reaction time which is consistent with a typical radical polymerization. The final yields of copolymerization also increase with the initiator concentration increasing. When the amount of AIBN is greater than 1.5 wt%, the initiator concentration has little effect on the final yields of the reaction, which are close to 90%. Fig. 6(b) shows the effect of the monomer concentrations on the yields. With the increase of monomer concentrations, the conversion rates of the reactions are significantly improved. When the monomer concentrations

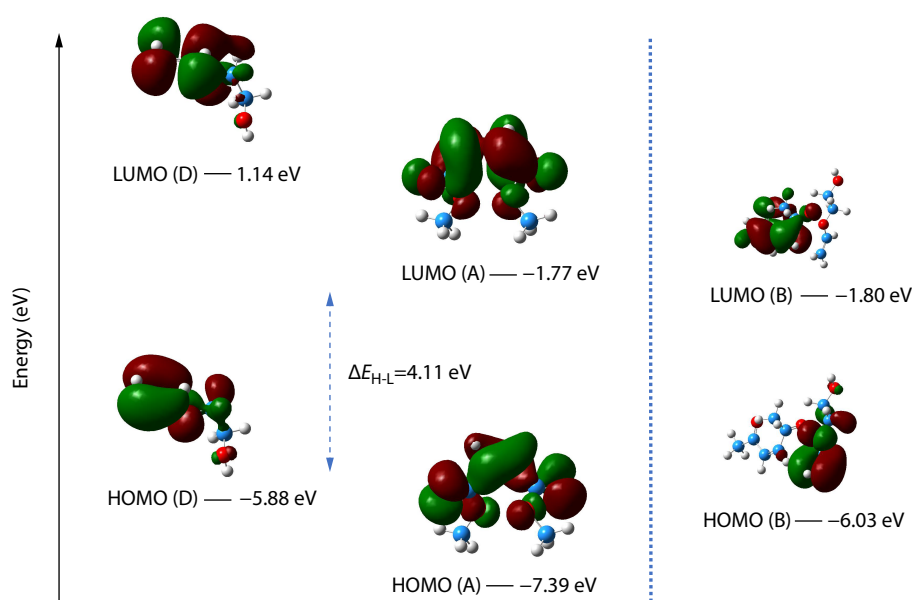


**Fig. 4** Donor (D), acceptor (A) and two monomers blending (B) localized HOMO and LUMO are shown. HOMO-LUMO gap ( $\Delta E_{H-L}$ ) is also indicated. All energies are in eV.

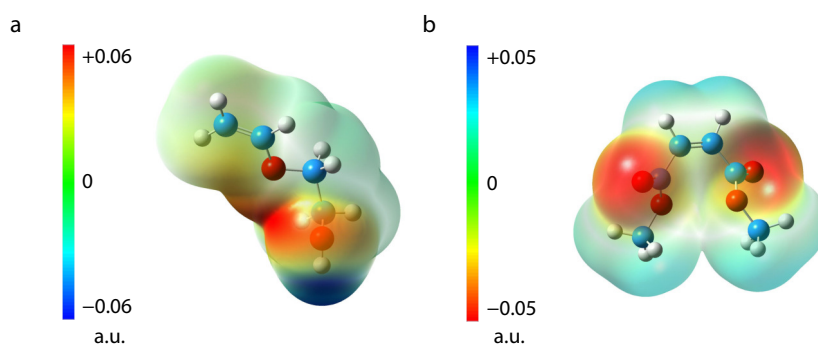


**Fig. 5** Molecular electrostatic potential surface (MEPS) of (a) HEVE and (b) DMM.

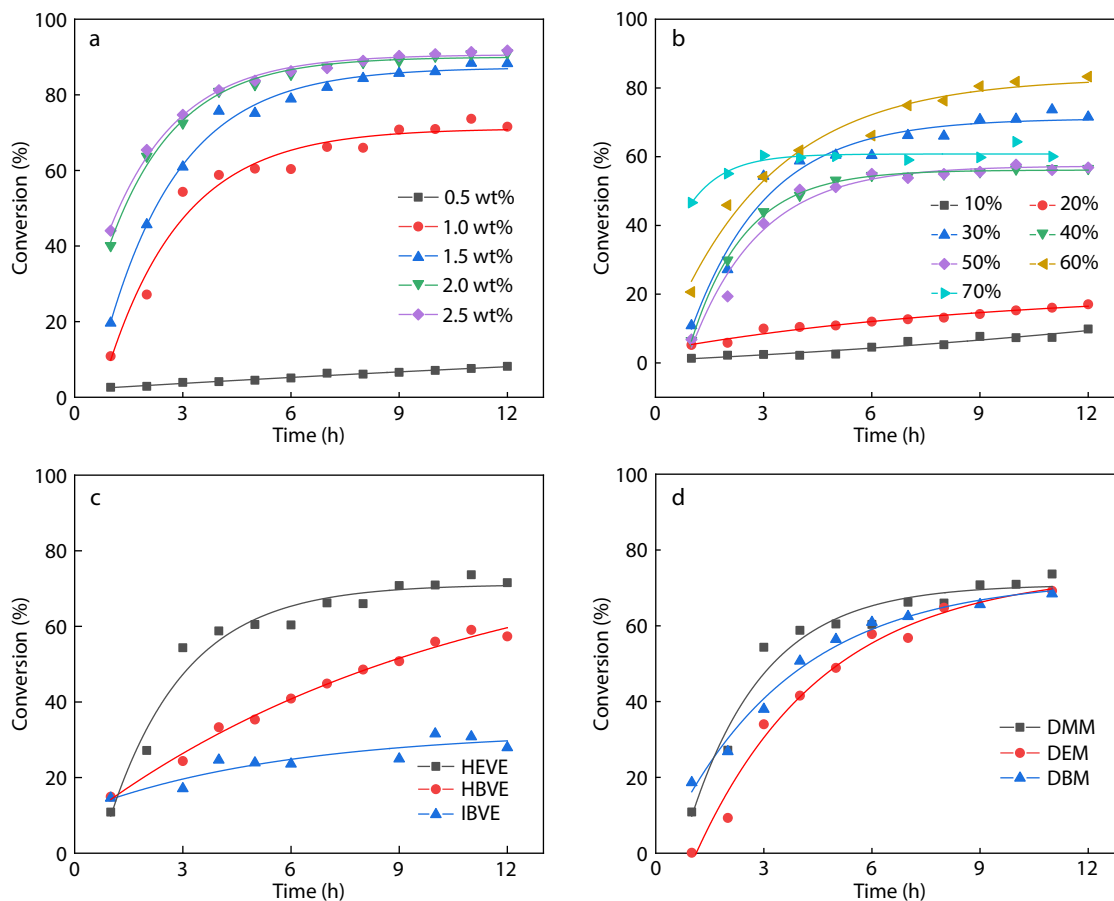


**Fig. 6** Curves of monomer conversions in (a) different initiator concentrations ( $[M_1]/[M_2]=1/1$ ), (b) different monomer concentrations (wt%), (c) different vinyl ethers (HEVE/HBVE/IBVE) with DMM, (d) different maleates (DMM/DEM/DBM) with HEVE.

are low (10 wt% and 20 wt%), the polymerization yields are less than 10%. At the lower monomer concentrations, the initiator concentrations in the reactants are also low, and the conversions of the reactions are greatly affected. When the monomer concentration is 70%, the copolymerization was very fast and almost completed within 1 h. This is mainly because the monomer concentrations are high, the viscosity of the reactant is high at the later stage and makes the diffuse of the monomers and propagating chains difficult.

Fig. 6(c) compares three vinyl ethers, namely HEVE, HBVE and IBVE. The overall yields of polymers decrease in the order of HEVE, HBVE and IBVE. The copolymerization of IBVE is much lower than those of HEVE and HBVE. Both HEVE and HBVE have hydroxyl groups which increase the electron density of vinyl ether and could form hydrogen bonds to boost the polymerization reactivity, comparing with IBVE.<sup>[5,12,14]</sup> The difference between HEVE and HBVE conversion is mainly due to the steric hindrance of the pendant groups. HEVE possesses a smaller steric hindrance and thus leading to a higher monomer conversion.<sup>[14]</sup>

As shown in Fig. 6(d), the differences of DMM, DEM and DBM are relatively small. This is due to the alkyl groups of different maleates have no significant difference in the electron effect and the reactivity of the monomers. The small difference is due to the steric hindrance. In the case of long alkyl substituents of maleates, the molecular chains of copolymers

synthesized with vinyl ethers and maleates possess large configuration (steric hindrance), which hinders the addition of maleates to the chain propagating species. Therefore, the conversion of maleates with long alkyl chains is lower than that of lower maleates.

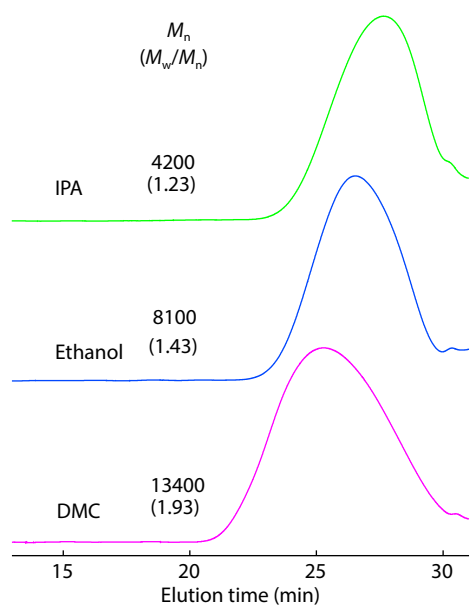
#### Effect on molecular weight

Table 1 summarizes the effect of the concentration and type of radical initiators, chain transfer agents, and solvents on the molecular weights of the produced copolymers. The results indicate that the initiator concentration has little effect on the molecular weight of the produced copolymers. The molecular weight of copolymer with BPO as initiator is smaller than that of AIBN at the similar reaction conditions. With the rise of the reaction temperature, the effect of side reactions, such as coupling and disproportionation terminations, is also increased. Thiol chain transfer agent has a certain effect on the molecular weight, but it is not as effective as the IPA and ethanol.

Fig. 7 shows the changes of molecular weight and molecular weight distribution of copolymers synthesized in different solvents (monomer concentration and initiator concentration are 30 wt% and 1.0 wt%, respectively). Obviously, under the similar conditions, the reaction was sensitive to the type of solvent. When the solvents were DMC, ethanol and IPA, the molecular weights of the copolymers were 13400, 8100 and 4200, respectively. The molecular weights of the copolymers

**Table 1** Experimental conditions, molecular characteristics of the alternating copolymers.

Entry	M <sub>1</sub>	M <sub>2</sub>	M <sub>1</sub> /M <sub>2</sub>	Time (h)	Temperature (°C)	Initiator	Solvent	CTA	Conv. (%)	M <sub>n</sub>	M <sub>w</sub> /M <sub>n</sub>
1	HEVE	DMM	1/1	12	65	1%AIBN	DMC	/	73.7	13400	1.93
2	HEVE	DMM	1/1	12	65	5%AIBN	DMC	/	88.1	13500	1.55
3	HEVE	DMM	1/1	12	65	10%AIBN	DMC	/	89.1	13000	1.58
4	HEVE	DMM	1/1	12	80	1%BPO	DMC	/	72.1	8500	1.51
5	HEVE	DMM	1/1	12	65	1%AIBN	DMC	4%BME	78.4	9600	1.48
6	HEVE	DMM	1/1	12	65	1%AIBN	DMC	4%TGA	78.9	7600	1.61
7	HEVE	DMM	1/1	12	65	1%AIBN	Ethanol	/	82.2	8100	1.43
8	HEVE	DMM	1/1	12	65	1%AIBN	IPA	/	75.1	4200	1.23

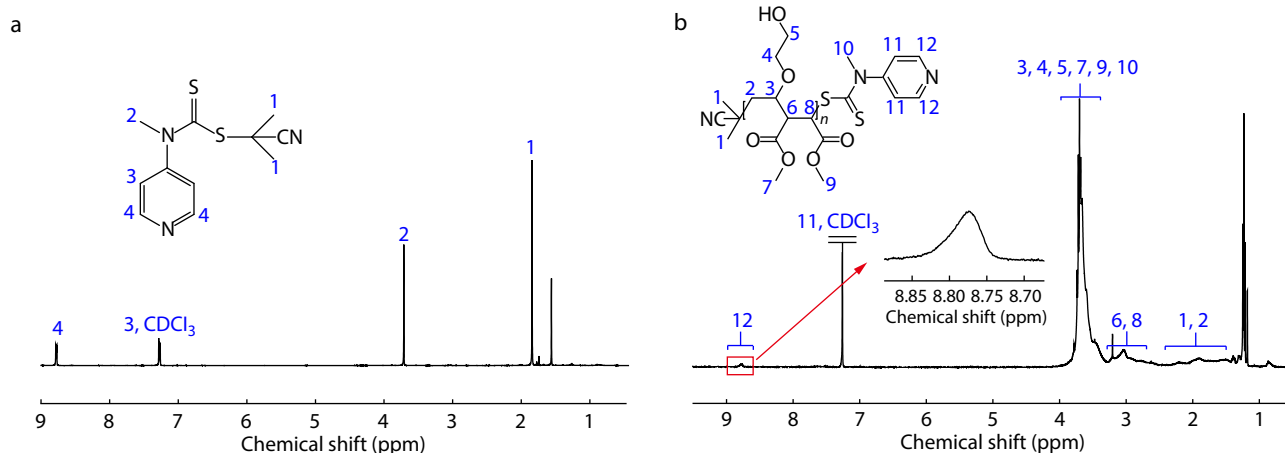
**Fig. 7** GPC traces of copolymers with the initial ratio of 1/1.

obtained in alcohols were lower than those obtained in DMC. At first, the chain transfer constants of the solvent in the order of IPA>ethanol>DMC. The second, the amount of effective hydrogen bond between molecule and solvent significantly determines the extent of reaction.<sup>[33]</sup> OH-VEs and alcohol solvents (ethanol and IPA) are easy to form intermolecular hydrogen bond, which reduces reactivity of the growing radical. Meanwhile, the formation of hydrogen bonding

between vinyl ether and solvent reduces the electron-donating capability of the vinyl ethers significantly. For the reasons, the OH-VE electron donating capability is weakened and the molecular weight of the copolymer decreases.

### RAFT Radical Copolymerization of HEVE and DMM

RAFT agent and poly(HEVE-*alt*-DMM) prepared by RAFT radical copolymerization were analyzed by <sup>1</sup>H-NMR (Fig. 8). The RAFT agent exhibited signals attributable to the methyl protons (1) due to the R group of RAFT agent, the methyl directly connected to nitrogen in Z group (2), and protons on pyridine (3 and 4) (the peak at 1.56 ppm belongs to water in CDCl<sub>3</sub>). Firstly, the <sup>1</sup>H-NMR spectrum of poly(HEVE-*alt*-DMM) prepared by RAFT radical copolymerization (Fig. 8b) is consistent with that of copolymer prepared by conventional radical polymerization (Fig. 2a) from 1.44 ppm to 4.00 ppm. This indicates that the copolymer prepared by RAFT polymerization has the similar alternating structure with the conventional radical polymerization. Secondly, in Fig. 8(b), the signal at 8.81 ppm attributes to the protons of pyridine moiety which was originated from the RAFT agent. The copolymers prepared by RAFT polymerization are typically terminated with RAFT agent. The interval values between adjacent fragments in Fig. S9 (in ESI) are respectively similar to the theoretical molecular weights of HEVE and DMM monomers. Combine Fig. S8 with Fig. S9, when the polymerization degree of the copolymer is 12 (*n*=12), the theoretical molecular weight of the copolymer is 2786.88 Da, and the experimental value is 3148.16 Da, which is 361.28 Da more than the theoretical value. The difference of 361.28 Da is the sum of the  $-(CH_3)_2C(CN)-$  fragment of the initiator AIBN or the R group of RAFT agent, the structure of the RAFT agent

**Fig. 8** (a) <sup>1</sup>H-NMR spectrum of the RAFT agent; (b) <sup>1</sup>H-NMR spectrum of the HEVE and DMM copolymer prepared by RAFT copolymerization.

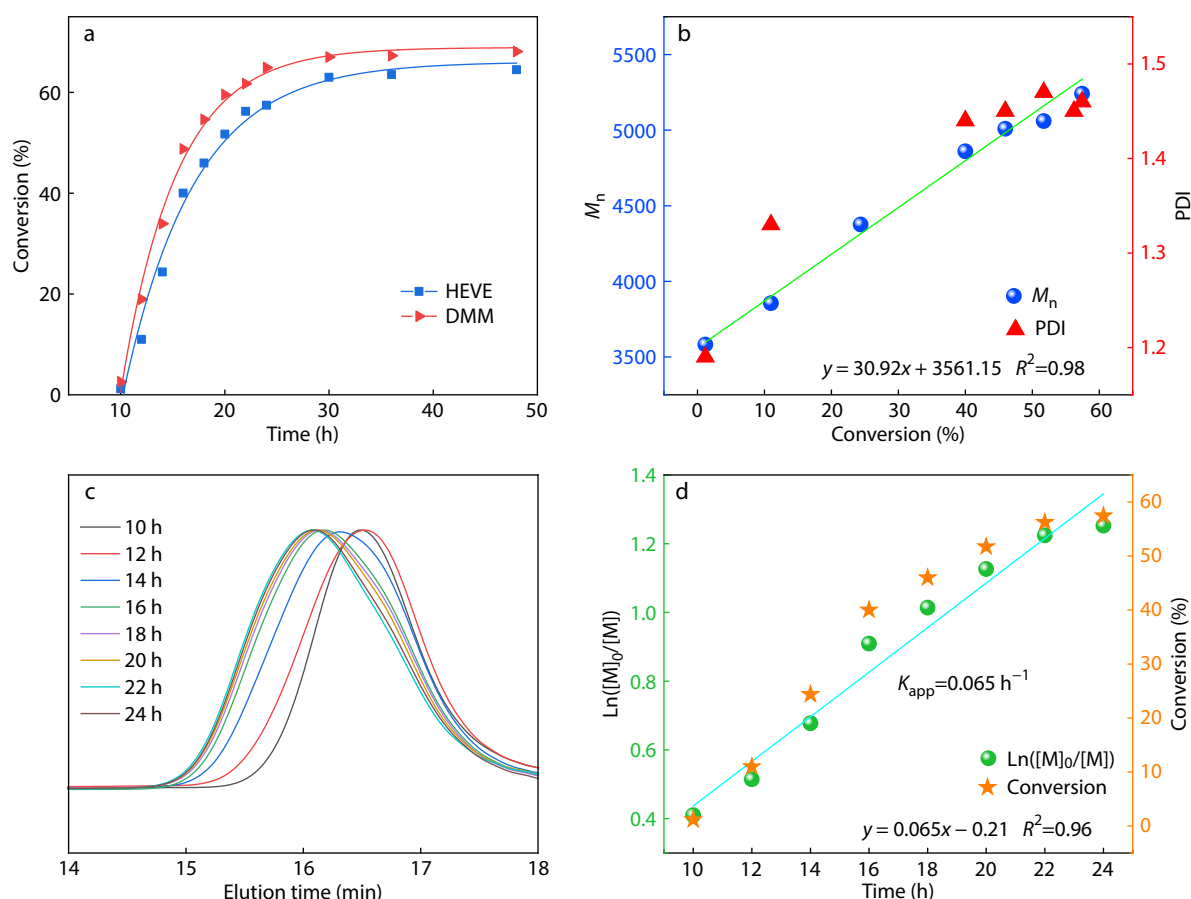


**Fig. 9** (a) Curves of monomer conversions; (b) Relations of  $M_n$  and  $M_w/M_n$  versus the monomer conversion:  $[\text{HEVE}]_0/[\text{DMM}]_0/[\text{RAFT agent}]_0/[\text{AIBN}]_0=100/100/3/1$ ; (c) GPC traces of copolymers with different reaction time; (d) Kinetics curves of copolymerization of HEVE and DMM.

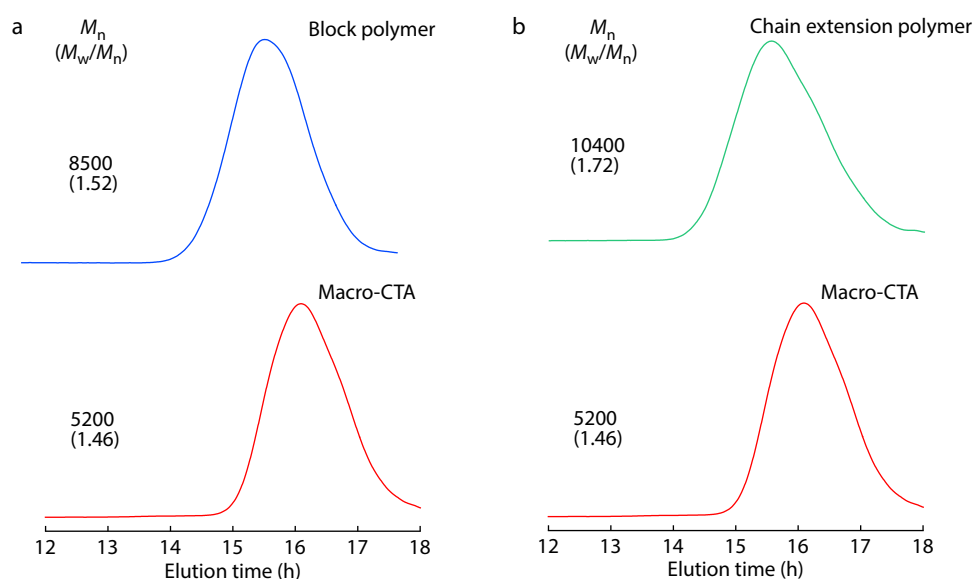
other than the R group,  $\text{Na}^+$  and a HEVE unit. It can be concluded that the copolymer with alternating structure was successfully prepared by RAFT polymerization.

Fig. 9 and Table S2 (in ESI) show the time-conversion curve of typical examples, the  $M_n$  and  $M_w/M_n$  of the copolymers as a function of monomer conversion, molecular weight versus time and kinetic curve of copolymerization. The time-conversion plot shows that HEVE was consumed at a close rate with DMM during the copolymerization as exactly as their reactivities in free radical copolymerization (Fig. 9a). As a whole, when the reaction proceeded for 24 h, the conversion entered a plateau and no longer increased significantly. Fig. 9(b) shows that the experimental  $M_n$  values are in direct proportion to the total monomer conversions. The  $M_w/M_n$  value increases with the conversion but as a whole remains in a controlled narrow range. The GPC evolution curves are all unimodal and consistently shift to a higher molecular end (Fig. 9c). Fig. 9(d) shows that the RAFT copolymerization of HEVE and DMM fits the first-order kinetic characteristics well. All the results verify that the use of 2-cyanopropan-2-yl *N*-methyl-*N*-(pyridin-4-yl)carbomdithioate as a RAFT agent successfully achieved controlled/living radical alternating copolymerization of HEVE and DMM. The effect of solvent on the RAFT copolymerization was also investigated (Fig. S10 in ESI). In DMC and ethanol, the  $M_n$  of obtained copolymers increased with

the monomer conversions but in IPA. This is also related to the higher chain transfer constant of IPA.

### Chain Extension and Block Copolymerization Using Poly(HEVE-*alt*-DMM) as Macro-CTA

To further demonstrate the fidelity of the poly(HEVE-*alt*-DMM), the chain extension and block copolymerization of VAc were conducted with poly(HEVE-*alt*-DMM) as macro-CTA ( $M_n=5200$  and  $M_w/M_n=1.46$ ). The GPC traces of the final products of both chain extension and block copolymerization move towards higher molecular ends compared with poly(HEVE-*alt*-DMM) macro-CTA (Fig. 10). The GPC elution curves are unimodal peaks, without evidence of low molecular weight fraction corresponding to the macro-CTA supported the high reinitiating efficiency and high end-group fidelity of the poly(HEVE-*alt*-DMM) macro-CTA. To the chain extension, molecular weight increased to  $M_n=10400$ , and  $M_w/M_n=1.72$ . The increasing of  $M_w/M_n$  is mainly due to the relatively poor control of the RAFT agent on the copolymerization of HEVE and DMM. The block polymerization showed a significant molecular weight increase ( $M_n=8500$ ) and a very slight increase of  $M_w/M_n=1.52$ . Fig. 11 shows the  $^1\text{H-NMR}$  spectrum of the poly(HEVE-*alt*-DMM)-*b*-poly(VAc). Chemical shift at 4.43 ppm (11) is attributed to VAc repeating units supported the successful preparation of the block copolymer.



**Fig. 10** GPC traces of (a) macro-CTA and block polymer, (b) macro-CTA and chain extension polymer.

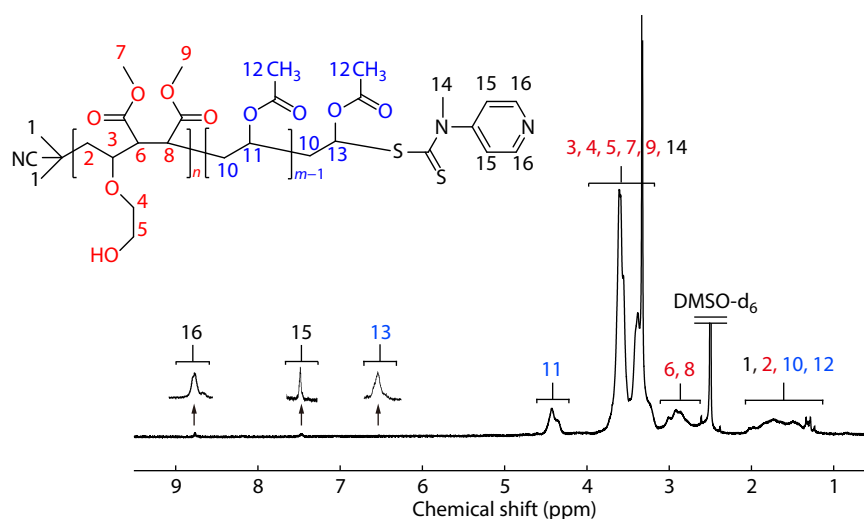


**Fig. 11**  $^1\text{H-NMR}$  spectrum of the poly(HEVE-*alt*-DMM)-*b*-poly(VAc).

## CONCLUSIONS

The alternating copolymerization of vinyl ethers and maleates are studied by conventional radical and RAFT polymerizations. In particular, the alternating structure of copolymer was demonstrated by NMR, MALDI-TOF MS and the monomer reactivity ( $r_1(\text{HEVE})=0.11\pm 0.07$ ,  $r_2(\text{DMM})=0.24\pm 0.10$ , and the product of  $r_1 \times r_2 = 0.026$ ). DFT calculations supported that HEVE and DMM have the nature of electron donor and acceptor to form alternating copolymer. The parameters of experiment such as monomer feeding ratio, monomer type, monomer concentration and others were used to analyse the influence on the copolymer structure. In addition, RAFT copolymerization of HEVE and DMM was developed using 2-cyanopropan-2-yl *N*-methyl-*N*-(pyridin-4-yl)carbomodithioate as an efficient RAFT agent. Poly(HEVE-*alt*-DMM) possessed a narrow molecular

weight distribution range ( $M_n=5200$  and  $M_w/M_n=1.46$ ). With the poly(HEVE-*alt*-DMM) as macro-CTA, both the chain extension with HEVE and DMM ( $M_n=10400$  and  $M_w/M_n=1.72$ ) and block copolymerization with VAc were successfully synthesized ( $M_n=8500$  and  $M_w/M_n=1.52$ ). This study provides a method for preparing and tailoring various copolymers of hydroxyalkyl vinyl ethers and alkyl maleates. In addition, it also offers a strategy how to exploit the 1,2-disubstituted ethylene in synthesis reactive polymers.

## Conflict of Interests

Wan-Tai Yang is an editorial board member for *Chinese Journal of Polymer Science* and was not involved in the editorial review or the decision to publish this article. All authors declare that there are no competing interests.

## **E** Electronic Supplementary Information

Electronic supplementary information (ESI) is available free of charge in the online version of this article at <http://doi.org/10.1007/s10118-023-2989-0>.

## ACKNOWLEDGMENTS

This work was financially supported by the National Natural Science Foundation of China (No. 22171017).

## REFERENCES

- Odian, G. in *Principles of Polymerization*, 4<sup>th</sup> Ed., John Wiley & Sons, Hoboken, New Jersey, **2004**, p. 198–349.
- Fueno, T.; Kamachi, M. Ab initio SCF study of the addition of the methyl radical to vinyl compounds. *Macromolecules* **1988**, *21*, 908–912.
- Kamachi, M.; Tanaka, K.; Kuwae, Y. ESR studies on radical polymerization of vinyl ethers. *J. Polym. Sci., Part A: Polym. Chem.* **1986**, *24*, 925–929.
- Miyamoto, M.; Ishii, T.; Sakai, T.; Kimura, Y. Radical polymerization of oligoethylene glycol methyl vinyl ethers in protic polar solvents. *Macromol. Chem. Phys.* **1998**, *199*, 119–125.
- Sugihara, S.; Kawamoto, Y.; Maeda, Y. Direct radical polymerization of vinyl ethers: reversible addition-fragmentation chain transfer polymerization of hydroxy-functional vinyl ethers. *Macromolecules* **2016**, *49*, 1563–1574.
- Matsumoto, A.; Nakana, T.; Oiwa, M. Radical polymerization of butyl vinyl ether. *Makromol. Chem., Rapid Commun.* **1983**, *4*, 277–279.
- Tran-Do, M. L.; Habas, J. P.; Ameduri, B. Oxygen-tolerant alternating copolymerization of fluorinated monomers and vinyl ethers at mild temperature. *ACS Appl. Polym. Mater.* **2022**, *4*, 1401–1410.
- Miyamoto, M.; Sawamoto, M.; Higashimura, T. Living polymerization of isobutyl vinyl ether with hydrogen iodide/iodine initiating system. *Macromolecules* **1984**, *17*, 265–268.
- Kamigaito, M.; Sawamoto, M. Synergistic advances in living cationic and radical polymerizations. *Macromolecules* **2020**, *53*, 6749–6753.
- Knutson, P. C.; Teator, A. J.; Varner, T. P.; Kozuszek, C. T.; Jacky, P. E.; Leibfarth, F. A. Brønsted acid catalyzed stereoselective polymerization of vinyl ethers. *J. Am. Chem. Soc.* **2021**, *143*, 16388–16393.
- Teator, A. J.; Leibfarth, F. A. Catalyst-controlled stereoselective cationic polymerization of vinyl ethers. *Science* **2019**, *363*, 1439–1443.
- Sugihara, S.; Yoshida, A.; Kono, T.-a.; Takayama, T.; Maeda, Y. Controlled radical homopolymerization of representative cationically polymerizable vinyl ethers. *J. Am. Chem. Soc.* **2019**, *141*, 13954–13961.
- Liao, Q.; Chen, D.; Zhang, X.; Ma, Y.; Zhao, C.; Yang, W. UV-assisted Li<sup>+</sup>-catalyzed radical grafting polymerization of vinyl ethers: A new strategy for creating hydrolysis-resistant and long-lived polymer brushes as a “smart” surface coating. *Langmuir* **2021**, *37*, 4102–4111.
- Duan, J.; Gong, Y.; Chen, D.; Ma, Y.; Song, C.; Yang, W. Radical homopolymerization of vinyl ethers activated by Li<sup>+</sup>- $\pi$  complexation in the presence of CH<sub>3</sub>OLi and Lil. *Polym. Chem.* **2022**, *13*, 1098–1106.
- Hao, X.; Fujimori, K.; Tucker, D. J.; Henry, P. C. An NMR determination of linkage configuration and monomer unit triad distribution in the copolymer of isobutyl vinyl ether and maleic anhydride. *Eur. Polym. J.* **2000**, *36*, 1145–1150.
- Ha, N. T. H.; Fujimori, K.; Henry, P. C.; Tucker, D. J. Assignment of <sup>13</sup>C NMR chemical shift and microstructure of copolymers of 2-chloroethyl vinyl ether-maleic anhydride and *n*-butyl vinyl ether-maleic anhydride. *Polym. Bull.* **1999**, *43*, 81–85.
- Braun, D.; Hu, F. Polymers from non-homopolymerizable monomers by free radical processes. *Prog. Polym. Sci.* **2006**, *31*, 239–276.
- Ng, L. T.; Nguyen, D.; Adeloju, S. B. Photoinitiator-free UV grafting of styrene, a weak donor, with various electron-poor vinyl monomers to polypropylene film. *Polym. Int.* **2005**, *54*, 202–208.
- Xu, C.; Chen, C.; Jiang, J.; Zhao, C.; Ma, Y.; Yang, W. Monodisperse styrene-maleic anhydride-isoprene terpolymer microspheres with tunable crosslinking density prepared by self-stabilized precipitation polymerization. *ACS Appl. Polym. Mater.* **2022**, *4*, 7363–7372.
- Gaylord, N. G.; Maiti, S.; Patnaik, B. K.; Takahashi, A. Donor-acceptor complexes in copolymerization. XXXVI. Alternating diene-dienophile copolymers. 4. Copolymerization of furan and 2-methylfuran with maleic anhydride. *J. Macromol. Sci., Part A-Chem.* **1972**, *6*, 1459–1480.
- Qiu, G. M.; Zhu, B. K.; Xu, Y. Y.; Geckeler, K. E. Synthesis of ultrahigh molecular weight poly(styrene-*alt*-maleic anhydride) in supercritical carbon dioxide. *Macromolecules* **2006**, *39*, 3231–3237.
- Rätzsch, M.; Vogl, O. Radical copolymerization of donor/acceptor monomers. *Prog. Polym. Sci.* **1991**, *16*, 279–301.
- Hawker, C. J., in *Handbook of Radical Polymerization*, 1<sup>st</sup> Ed., John Wiley & Sons, Hoboken, New Jersey, **2002**, p. 463–521.
- Matyjaszewski, K. Atom transfer radical polymerization (ATRP): current status and future perspectives. *Macromolecules* **2012**, *45*, 4015–4039.
- Tang, W.; Matyjaszewski, K. Effect of ligand structure on activation rate constants in ATRP. *Macromolecules* **2006**, *39*, 4953–4959.
- Tang, W.; Tsarevsky, N. V.; Matyjaszewski, K. Determination of equilibrium constants for atom transfer radical polymerization. *J. Am. Chem. Soc.* **2006**, *128*, 1598–1604.
- Chiefari, J.; Chong, Y. K.; Ercole, F.; Krstina, J.; Jeffery, J.; Le, T. P. T.; Mayadunne, R. T. A.; Meijs, G. F.; Moad, C. L.; Moad, G.; Rizzardo, E.; Thang, S. H. Living free-radical polymerization by reversible addition-fragmentation chain transfer: the RAFT process. *Macromolecules* **1998**, *31*, 5559–5562.
- Hawthorne, D. G.; Moad, G.; Rizzardo, E.; Thang, S. H. Living radical polymerization with reversible addition-fragmentation chain transfer (RAFT): direct ESR observation of intermediate radicals. *Macromolecules* **1999**, *32*, 5457–5459.
- Mayadunne, R. T. A.; Jeffery, J.; Moad, G.; Rizzardo, E. Living free radical polymerization with reversible addition-fragmentation chain transfer (RAFT polymerization): approaches to star polymers. *Macromolecules* **2003**, *36*, 1505–1513.
- Zhang, Z.; Hong, L.; Gao, Y.; Zhang, W. One-pot synthesis of POSS-containing alternating copolymers by RAFT polymerization and their microphase-separated nanostructures. *Polym. Chem.* **2014**, *5*, 4534–4541.
- You, Y.-Z.; Hong, C. Y.; Pan, C. Y. Controlled alternating copolymerization of St with MAH in the presence of DBTTC. *Eur. Polym. J.* **2002**, *38*, 1289–1295.
- Lee, H.; Pack, J. W.; Wang, W.; Thurecht, K. J.; Howdle, S. M. Synthesis and phase behavior of CO<sub>2</sub>-soluble hydrocarbon copolymer: poly(vinyl acetate-*alt*-dibutyl maleate). *Macromolecules* **2010**, *43*, 2276–2282.
- Sugihara, S.; Yoshida, A.; Fujita, S.; Maeda, Y. Design of hydroxy-functionalized thermoresponsive copolymers: improved direct

- radical polymerization of hydroxy-functional vinyl ethers. *Macromolecules* **2017**, *50*, 8346–8356.
- 34 Puts, G.; Venner, V.; Améduri, B.; Crouse, P. Conventional and RAFT copolymerization of tetrafluoroethylene with isobutyl vinyl ether. *Macromolecules* **2018**, *51*, 6724–6739.
- 35 Zhang, C.; Chen, D.; Yang, W. Preparation of styrene-maleic anhydride-acrylamide terpolymer particles of uniform size and controlled composition *via* self-stabilized precipitation polymerization. *Ind. Eng. Chem. Res.* **2020**, *59*, 15087–15097.
- 36 Wang, Y.; Zhang, X.; Ma, Y.; Chen, D.; Zhao, C.; Yang, W. Polythioethers with controlled  $\alpha,\omega$ -end groups prepared by visible light induced thiol-ene click polymerization of dithiol and divinyl ether with 4-(*N,N*-diphenylamino)benzaldehyde as organocatalyst. *Macromol. Chem. Phys.* **2020**, *221*, 1900557.
- 37 Zografos, A.; Lynd, N. A.; Bates, F. S.; Hillmyer, M. A. Impact of macromonomer molar mass and feed composition on branch distributions in model graft copolymerizations. *ACS Macro Lett.* **2021**, *10*, 1622–1628.
- 38 Fineman, M.; Ross, S. D. Quantitative investigation of X-ray diffraction by “amorphous” polymers and some other noncrystalline substances. *J. Polym. Sci.* **1950**, *5*, 269–281.
- 39 Beckingham, B. S.; Sanoja, G. E.; Lynd, N. A. Simple and accurate determination of reactivity ratios using a nonterminal model of chain copolymerization. *Macromolecules* **2015**, *48*, 6922–6930.
- 40 Cui, Z. H.; Aquino, A. J. A.; Sue, A. C. H.; Lischka, H. Analysis of charge transfer transitions in stacked  $\pi$ -electron donor-acceptor complexes. *Phys. Chem. Chem. Phys.* **2018**, *20*, 26957–26967.
- 41 Ahmed, R.; Manna, A. K. Molecular-scale engineering of the charge-transfer excited states in non-covalently bound Zn-porphyrin and carbon fullerene based donor-acceptor complex. *Phys. Chem. Chem. Phys.* **2020**, *22*, 14822–14831.
- 42 Duva, G.; Pithan, L.; Zeiser, C.; Reisz, B.; Dieterle, J.; Hofferberth, B.; Beyer, P.; Bogula, L.; Opitz, A.; Kowarik, S.; Hinderhofer, A.; Gerlach, A.; Schreiber, F. Thin-film texture and optical properties of donor/acceptor complexes. Diindenoperylene/F6TCNNQ vs alpha-sexithiophene/F6TCNNQ. *J. Phys. Chem. C* **2018**, *122*, 18705–18714.
- 43 Ushakov, E. N.; Martyanov, T. P.; Vedernikov, A. I.; Efremova, A. A.; Moiseeva, A. A.; Kuz'mina, L. G.; Dmitrieva, S. N.; Howard, J. A. K.; Gromov, S. P. Highly stable supramolecular donor-acceptor complexes involving a bis(18-crown-6)azobenzene as weak donor: structure-property relationships. *ACS Omega* **2020**, *5*, 25993–26004.
- 44 Zhang, B.; Qian, B. B.; Li, C. T.; Li, X. W.; Nie, H. X.; Yu, M. H.; Chang, Z. Donor-acceptor systems in metal-organic frameworks: design, construction, and properties. *CrystEngComm* **2022**, *24*, 5538–5551.
- 45 Khan, E.; Shukla, A.; Srivastava, A.; Shweta; Tandon, P. Molecular structure, spectral analysis and hydrogen bonding analysis of ampicillin trihydrate: a combined DFT and AIM approach. *New J. Chem.* **2015**, *39*, 9800–9812.
- 46 Fukui, K. Role of frontier orbitals in chemical reactions. *Science* **1982**, *218*, 747–754.
- 47 Fukui, K.; Yonezawa, T.; Shingu, H. A molecular orbital theory of reactivity in aromatic hydrocarbons. *J. Chem. Phys.* **1952**, *20*, 722–725.
- 48 Issa, Y. M.; Abdel-Latif, S. A.; El-Ansary, A. L.; Hassib, H. B. The synthesis, spectroscopic characterization, DFT/TD-DFT/PCM calculations of the molecular structure and NBO of the novel charge-transfer complexes of pyrazine Schiff base derivatives with aromatic nitro compounds. *New J. Chem.* **2021**, *45*, 1482–1499.
- 49 Lewis, D. F. V.; Lake, B. G.; Ioannides, C.; Parke, D. V. Inhibition of rat hepatic aryl hydrocarbon hydroxylase activity by a series of 7-hydroxy coumarins: QSAR studies. *Xenobiotica* **1994**, *24*, 829–838.
- 50 Bora, S. R.; Kalita, D. J. Hopping transport in perylene diimide based organic solar cells: a DFT approach. *New J. Chem.* **2022**, *46*, 19357–19372.